Eurographics Workshop on Visual Computing for Biology and Medicine (2017)
S. Bruckner, A. Hennemuth, and B. Kainz (Editors)

HIFUtk: Visual Analytics for High Intensity Focused Ultrasound Simulation

D. Modena[1], E. van Dijk[2], D. Bošnački[1], H.M.M. ten Eikelder[1] and M.A. Westenberg[2]

[1]Department of Biomedical Engineering, Eindhoven University of Technology, The Netherlands
[2]Department of Mathematics and Computer Science, Eindhoven University of Technology, The Netherlands

Abstract

Magnetic Resonance-guided High Intensity Focused Ultrasound (MR-HIFU) is a novel and non-invasive therapeutic method. It can be used to locally increase the temperature in a target position in the human body. HIFU procedures are helpful for the treatment of soft tissue tumors and bone metastases. In vivo research with HIFU systems poses several challenges, therefore, a flexible and fast computer model for HIFU propagation and tissue heating is crucial. We introduce HIFUtk, a visual analytics environment to define, perform, and visualize HIFU simulations. We illustrate the use of HIFUtk by applying HIFU to a rabbit bone model, focusing on two common research questions related to HIFU. The first question concerns the relation between the ablated region shape and the focal point position, and the second one concerns the effect of shear waves on the temperature distribution in bone. These use cases demonstrate that HIFUtk provides a flexible visual analytics environment to investigate the effects of HIFU in various type of materials.

Categories and Subject Descriptors (according to ACM CCS): I.3.8 [Computer Graphics]: Applications—

1. Introduction

Magnetic Resonance-guided High Intensity Focused Ultrasound (MR-HIFU) is a novel and non-invasive therapeutic method which has emerged in the last decade. MR-HIFU enables the rapid heating of a specific part in the body (focal point), and consequent coagulative necrosis (cell death) [Haa11]. The temperature increase in the target position is induced by the ultrasound focused beam, generated by a set of oriented transducer elements. An explanation of HIFU treatment is shown in Figure 1. Herein, MR thermometry using proton resonance frequency shift (PRFS) [SQM05] is used to plan, follow, and evaluate the HIFU procedure. The PRFS method can be applied to water-rich tissue, like uterine fibroids, but it fails in water-poor tissue like bone.

It has been demonstrated that HIFU procedures are helpful for the treatment of soft tissue tumors like uterine fibroids, as well as for bone metastases [SBD*13]. HIFU treatments for uterine fibroids are associated with a reduction of the tumor size [VFW*00, SRT*06], maintaining a high safety profile [SRT*06, SGT*03]. General treatments for bone metastases are palliative, focused on alleviating the pain associated with the presence of metastases, which compromise the quality of life of the patient. HIFU procedures are a promising method, technically feasible [HLB*14], able to achieve pain relief [HLB*14, NAM*13], and tumor control [NAM*13].

Experimental research with HIFU systems poses several challenges. First, experiments using HIFU systems are time-consuming. Further, researchers face technical problems, for instance, repeated heating of the tissue-mimicking gel causes fast degradation of the material, limiting its use. Finally, the results of an experiment are strongly influenced by the initial parameters of the system (e.g. the position of the transducer elements, the initial power, the electronic steering applied).

A flexible and fast model for HIFU propagation, valid in soft tissue and bone, is crucial for a researcher who wants to predict the temperature increase under different experimental configurations. Computer models for HIFU propagation can predict the location and the amount of energy deposition during the treatment. This is important for therapy planning in a clinical environment, but this is also relevant at the research level. Furthermore, using an *in silico* approach can overcome the limitations of the PRFS thermometry data, which can only be acquired in soft tissues. Also, the spatial resolution of the temperature map given by the PRFS thermometry is low compared to the dimension of the treatment region.

Aim: we propose HIFUtk to navigate, extract, and fully exploit the data and results from a HIFU Ray-tracer based computer model [EBE*16], which enables the temperature prediction both in soft tissues and in bone. HIFUtk enables the model to be more accessible to researchers, by improving the usability of the algorithms and the performance. Hence, the user is able to obtain results from HIFU simulation in seconds, avoiding dependencies on proprietary third party software, and can visually explore the simulation results.

DOI: 10.2312/vcbm.20171239

Contributions: we introduce a visual analytics environment for:

- Defining the experimental set-up in the simulation: material properties, system parameters (e.g. initial power, frequency) and geometry (both by primitives and by extracting CT-data).
- Running HIFU simulations with the possibility to extract and navigate intermediate and final results.
- Overcoming the difficulties of visualizing volumetric temporal data (e.g. the temperature evolution in a volume)

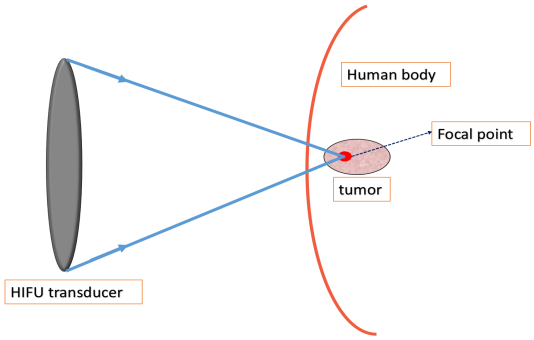

Figure 1: *HIFU treatment for soft tissue tumors. The transducer elements enable the ultrasound beam to be focused on a specific part of the body (the focal point). The US waves can be focused on a circular area with radius of 2, 4 or 8 mm. The increase of temperature due to the ultrasound waves interference leads to the ablation (removal) of the tumor.*

2. Related work

In this section we give an overview regarding models for ultrasound (US) propagation and visualization tools for pre-treatment planning for cancer treatments.

Modelling US waves in soft tissue is usually limited to the investigation of longitudinal US waves. In bone, which is a solid material, also shear US waves contribute to the increase of the temperature in the focal region [NM10]. In fact, it has been demonstrated that the heat generated by shear waves in bone cannot be neglected when the angle of incidence of US waves on an interface is oblique [CSG74].

The gold standard for simulating ultrasound propagation is solving the wave equation. Full-wave solvers are the finite-difference time-domain method (FDTD) [ATP*03] and the finite-element method [WMA*]. The high computation time and the huge memory requirements necessary are common features related to these methods.

Another general accepted approach is the angular spectrum plane wave (ASPW) method [Cob07], which can deal only with flat surfaces. Vyas et al. [VC12] proposed a hybrid angular spectrum method in order to simulate the propagation in more complex geometries. A stochastic Ray-tracing approach has been proposed by Koskela et al. [KVG*14]. This model is able to describe the longitudinal ultrasound waves but not the shear waves propagation.

In general, HIFU propagation in the presence of the interface tissue-bone has been investigated in various studies [LYL*00, HPKF12,SPS*13]. Shear waves propagation in bone has been studied as well [CSG74, LLC*00, NM10]. A common feature in the aforementioned methods is that the models can only deal with flat surfaces. It is therefore not possible to simulate US propagation on realistic bone shapes.

In the visualization literature, a description of HIFU propagation tools addressed to researchers is lacking.

Amin et al. [AWR*06] presented a systematic approach towards HIFU therapy planning. From this, an extended integrated software platform for HIFU simulations is described by Wu et al. [WARR07]. Tools for the segmentation, HIFU simulation (including a bio-heat equation solver) and visualization are integrated in their platform. The user is able to generate a 3D model from MRI/CT slices of the human body, apply HIFU simulation and evaluate the temperature evolution. As it is thought as a first step towards a system usable in a clinical environment, no information is present about the possibility for the user to complete tasks which are common for a researcher. Such tasks include, for instance, the extraction of intermediate results (such as the power produced in the focal region), the possibility to choose different solvers for the bio-heat equation or the visualization of the thermal dose output. Moreover details about the overall time for computing a complete simulation are lacking.

Scott et al. [SSP*14] provided an integrated model-based software for focused ultrasound application in moving abdominal organs due to the respiratory motion. It is not suitable for the treatment of bone metastases. Available general Matlab-based US simulation tools are k-wave [TJRC12] and HIFU_ Simulator [Son09].

More examples of pre-treatment tools addressed to a clinical enviroment for radiotherapy and radiofrequency can be found in the literature [ZJOB10, VSP*]. The main goal of such systems is to maximize the delivery of the treatment in the tumor region and minimize the damage to healthy tissue. Zhao et al. [ZJOB10] proposed an evaluation of the treatment plan based on different spatial and biological features. More relevant for our scope, Villard et al. [VSP*] present a simulation treatment tool for radiofrequency ablation. As this technique, contrary to HIFU procedures, is invasive, the main challenge of such a system is the definition of the correct trajectory of the needle inside the body.

3. Methods

A typical workflow [EBE*16] and the proposed one to simulate a HIFU experiment are shown in Figure 2.

In the typical workflow the user has to define the material parameters in which the US waves travel (e.g. attenuation coefficient, density, speed of sound) and the HIFU simulation parameters (e.g. frequency, initial power, transducer position, position of the focal point). In the same fashion, the geometry of the system (e.g. muscle thickness, bone position, bone inclination) has to be specified.

Once this first step is done, the user can proceed with the HIFU simulation, based on a Ray-tracer model [EBE*16] in MATLAB. The output of this method is not yet the temperature evolution, but

the power produced in the focal region $Q(x,y,z)$, which is used in the next phase as heat source for the solution of the heat equation.

The solution of the heat equation is computed with a finite element method in COMSOL, and the user has to re-define both the geometry and the material parameters. Once the heat equation is solved, the user is able to extract and analyse the data of the temperature evolution $T(x,y,z,t)$ in the region of interest.

From the temperature data, Cumulative Equivalent Minutes (CEM) quantification can be calculated. The CEM empirical formula [SD84] is defined as:

$$\int_{t_0}^{t_f} R^{T_{ref}-T}\,dt, \tag{1}$$

where T is the temperature and T_{ref} is a reference temperature (commonly 43°C). This is then integrated over time during the therapy from the start t_0 to end t_f. The parameter R has been derived empirically and can assume two values: 0.5 if $T \geq T_{ref}$ or 0.2 in the other cases. The ablation threshold for every material is CEM $= 400$, so if CEM ≥ 400, the ablation occurs.

This typical workflow presents many limitations, such as:

- The user has to define the same geometry and parameters in two different phases and systems
- The output of the Ray-tracer model has to be exported from the MATLAB environment and imported into COMSOL
- The definition of the geometry is based only on primitives, so it is impossible to deal with a complex geometry (e.g. from CT-data)

The new workflow implemented in HIFUtk enables the user to define the parameters and geometry only once, and in one step the HIFU simulation and the temperature evolution are computed. It is important to underline that the user can visualize, investigate and export both the power produced and the temperature data.

Moreover, the simulation can also be done only at the level of the Ray-tracer simulation, without solving the heat equation. This is important in case the user wants to compare the power production output from the Ray-tracer with the output from another US model. The proposed workflow consists of both a computational approach and a visualization approach.

3.1. Computational Approach

3.1.1. The Ray-tracer model

The Ray-tracer model [EBE*16] describes the acoustic power flowing from each transducer element by a number of rays of power, which randomly target the points inside a circle in the coronal plane (the plane perpendicular to the US beam). A graphic representation of the model in a simple muscle-bone-marrow configuration is shown in Figure 4.

Whenever a ray hits a material interface it can potentially split into a reflected and a transmitted one. In the case of fluid solid interfaces there is also a separate shear and longitudinal transmission (see Figure 3). At each interface, the transmission and reflection coefficient to adjust the power of the transmitted and reflected rays are calculated.

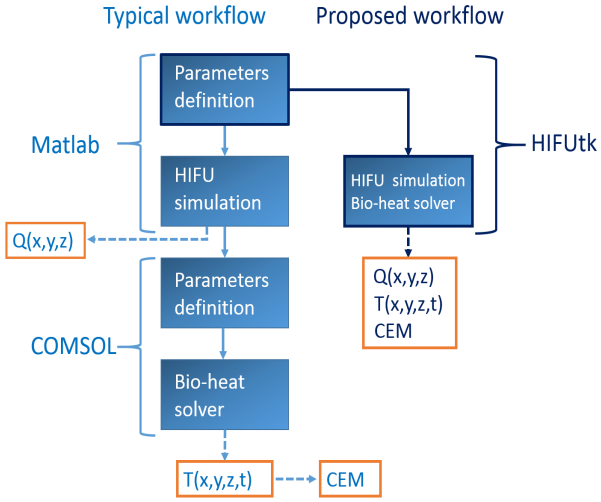

Figure 2: *A typical and the proposed workflow. HIFUtk provides a single system to define a simulation experiment, and visualize the intermediate and final results (heat production, temperature evolution and CEM).*

The first stage of the algorithm (segment collection) is the generation and storage of all the rays (refracted and reflected). Therefore, the output of the first stage of the algorithm is a set of rays, each having an origin, intersection point, initial intensity and end point intensity, and a single material. The next step (heat production phase) is to combine all of the ray-segments together to compute the heat production as a function of position in W/cm^3. Here the contribution of each ray is stored in a uniform grid with a certain cell size dx. To do so, ray-marching is used where small steps of size $\Delta d < dx$ along each ray are taken, where at each step the loss in intensity is stored in the nearest cell in the grid. The amount of energy deposited is the difference in intensity between two points in the discretization.

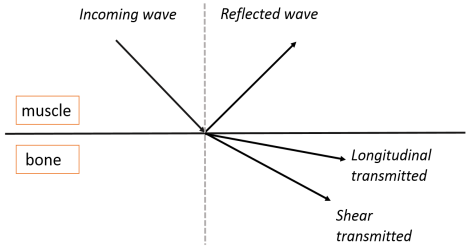

Figure 3: *Shear and longitudinal US waves contribute at the temperature increase in solid material, such as bone.*

3.1.2. The bio-heat equation solver

We used Finite Difference (FD) methods for solving the bio-heat equation. The user may need to solve the bio-heat equation using different solvers and boundary conditions according to the dimensions of the geometry. Hence, we developed a number of differ-

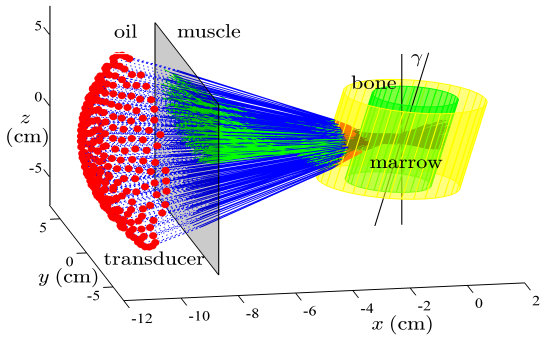

Figure 4: *Graphic representation of the model.*

ent solvers with varying degree of accuracy and different boundary conditions. The solvers available are *Explicit Euler*, *Implicit Euler*, *Crank-Nicolson*, *Explicit fourth-order*, *Implicit fourth-order* and *Alternating Direction Implicit Method (ADI)*. The user can choose between *Dirichlet* and *von Neumann* boundary conditions. For more details see [Tho95].

3.1.3. Optimization

An important requirement of HIFUtk is to allow the user to run the simulation in a reasonable amount of time. To achieve this goal, we introduce different optimizations both at the level of the Ray-tracer implementation and in the bio-heat equation solver. We optimised the Ray-tracer algorithm by using multi-threading in the segment collection and in the heat production phase. The multi-threaded approach was implemented both on CPU and GPU. In the case of 200 rays per transducer element, the Matlab implementation took about 1200 s to generate the heat production, while HIFUtk less than 2 s. To achieve a good performance, we use Bounding Volume Hierarchies (BHV) [KHM*98, LGS*09] and the closest intersection is found using a fast Ray-triangle intersection algorithm [MT05]. Regarding the bio-heat equation solver, we achieve the optimization using GPU and CPU implementation. The run-time obtained for the explicit method on a 32^3 grid with a time step of 0.005 s using the CPU (single threaded) is 1.9 s, using GPU implementation with multi-threading is 1.48 s and CPU implementation with multi-threading 0.82 s.

3.2. Visualization Approach

3.2.1. The Ray-tracer model visualization

We provide the Ray-tracer model visualization to facilitate the user in the investigation of the role of the different ray types in the volume. To do so, all the rays generated by the Ray-tracer algorithm can be shown in a 3D context, including the transducer elements. The user is not interested in the behaviour and the location of a single ray, but he may need information about the orientation and the behaviour of a group of rays. Therefore, in the ray visualization window each ray type has a distinct color and the user is able to visualize any of these independently. The view with all the ray types has been implemented for the sake of completeness, but it is rarely used by the user due to its complexity. Different plane views (coronal, sagittal and lateral slices) are provided to analyse the rays inside the geometry. Multiple Ray-tracer views are shown in Figure 5.

The user can interact with the Ray-tracer model visualization in different ways. The camera can be moved, and the user can zoom in the region of interest. Moreover, the objects can be rotated and the new rays pattern and the consequent heat production output are instantaneously re-computed and stored in the results variables. This is useful when the user wants to analyse the role of shear waves (strongly affected by the angle of intersection) at different inclination angles.

We also provide an animated visualization of the rays from the transducer elements till the end of the geometry. While playing the animation, the user is able to select the preferred velocity of the rays. This is useful to understand the details of reflection and refraction of the rays at each interface.

3.2.2. Simulation data visualization

There are three main simulation results the user is able to visualize: the produced power $Q(x,y,z)$ in the focal region, the CEM quantification and the temperature evolution $T(x,y,z,t)$. All results can be visualized in a 3D environment, but the user is able to cut slices, lines and points to move towards 2D and 1D views.

An effective 3D visualization of the results in HIFU simulation is crucial to get an overall idea about the treatment effect on the materials (bone/tissue mimicking gel). For instance, the user may be interested in assessing the dimension of the ablated region in the focal zone or the maximum temperature reached in the proximity of the bone. To combine translucent geometry with volume data, we make use of depth peeling algorithm [Eve01], which is an order independent transparency technique.

By default the application uses volume rendering and transparent meshes, it is however possible to show a shaded version with application of a lighting model. Besides visualising the volume also a surface representation of the scalar field can be visualised. The two remaining views show either the wire-frame to inspect the geometry, and a solid rendering. The user may be interested in obtaining information about a specific slice while inspecting 3D data-types, so slices automatically taken from the coronal, saggital and lateral planes are shown as well (see Figure 6).

For comparing HIFUtk results with other outputs we provide 2D views. For instance, common tasks are the comparison between the HIFUtk temperature output in the focal planes with the experimental PRFS thermometry output or between the Ray-tracer power production and the one from another model. In this case, it is fundamental that the color map of the 2D view in HIFUtk is the same as the one used in the other outputs. Height maps give a better sense of the relative amplitude of the data value in a specific point. Moreover the user can probe a specific data value by simply moving the mouse over a data point.

For temporal data comparison, we provide 1D data views. This is useful when experimental data from temperature sensors have to be compared with the model output data. As in the 3D and 2D views, the user can interact with the 1D data viewer, for example

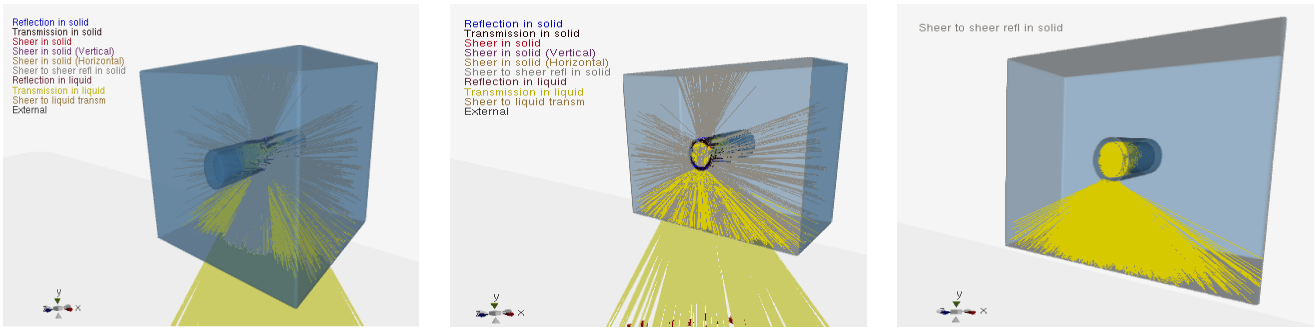

(a) (b) (c)

Figure 5: *Ray-tracer visualization showing the trajectory and type of the rays (a) and the lateral plane (b). Filtering of the ray-segments based on the type (c) is also possible. In order to avoid occlusion of the target region by the rays, the user can zoom into the geometry.*

the 1D view has the option to examine each data point by hovering the mouse over it. Moreover, different outputs can be displayed in the same plot. This is useful when the user wants to compare the temperature trend over time in different positions in bone (See Figure 7)

The visualization of temporal data-types is solved by the analysis tools where the maximum, minimum or average value can be shown. It is possible to define a sum or mathematical expression for an integral over time. The result at any specific time-interval can be shown by any of the previously described data-view components by selecting it from the list of available measurements. Besides picking a single time also a movie playback can be shown, which displays interpolated results over the calculated measurements.

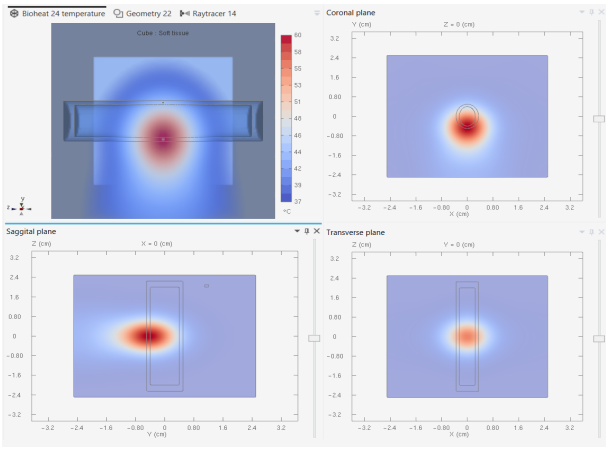

Figure 6: *Integration of 3D and 2D views. The slice selected in the 2D view is automatically shown in the 3D view as well. The dots in the bone in the 3D views are sensors point defined by the user. The user is able to investigate the temperature trend in these points (1D plot) in the data component of the system.*

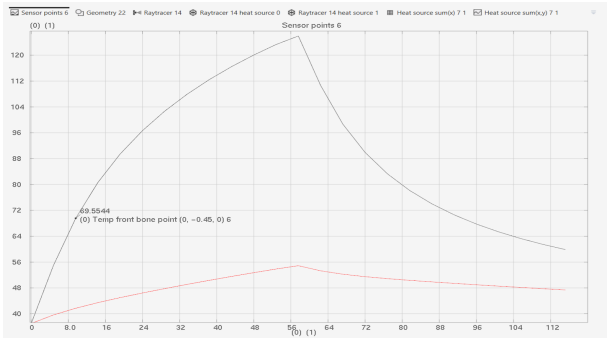

Figure 7: *1D view of the temperature trend of the sensor which position is shown in Figure 6. If the user hovers the mouse over the graph, the data value is automatically shown.*

4. HIFUtk tool

The general user interface for a typical experiment is shown in Figure 8. Here the orange highlighted area in the tool-bar is used to open, save and compute the current experiment. The red highlighted area contains all of the different components in an experiment subdivided into geometry, simulation, data and analysis. Whenever a component in this tree is selected its properties are shown in the property editor in blue. If such a component contains spatial data its view is shown in the green highlighted area. The pink toolbox dynamically shows all of the interaction and visualisation options for the currently selected view.

After configuring such an experiment, the solution can be computed using the *Compute* tool bar button shown in the orange rectangle in Figure 8.

5. Results

5.1. Performance

We assessed the performance of our approach on a PC with an Intel 3550k i5 processor and NVIDIA GeForce 660 GTX graphics processor (GPU). These can be classified as mid- to high-end hardware and represent a typical workstation. Figure 9 show timings

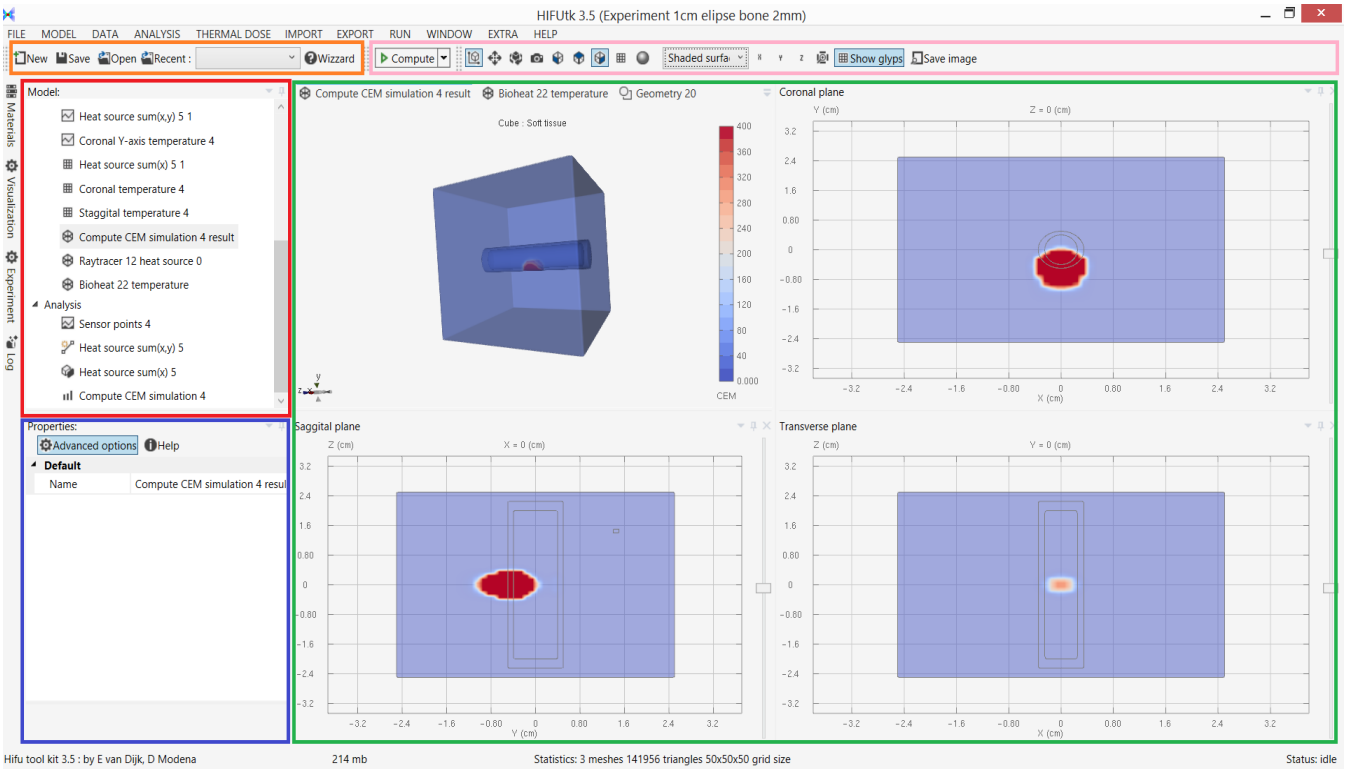

Figure 8: *Graphic User Interface. The orange highlighted area in the tool-bar is used to open, save and compute the current experiment. The red highlighted area contains all of the different components in an experiment subdivided into geometry, simulation, data and analysis. The property editor is in the blue highlighted area. If a component contains spatial data its view is shown in the green highlighted area. The pink toolbox shows all of the interaction and visualisation options for the currently selected view.*

obtained using the HIFUtk implementation. In these experiments the phantom case study is used which has a domain of 15 cm in each dimension with a cell size of 0.1 cm leading to a heat production of 150^3 elements. This does not include any visualisation or exporting of the results.

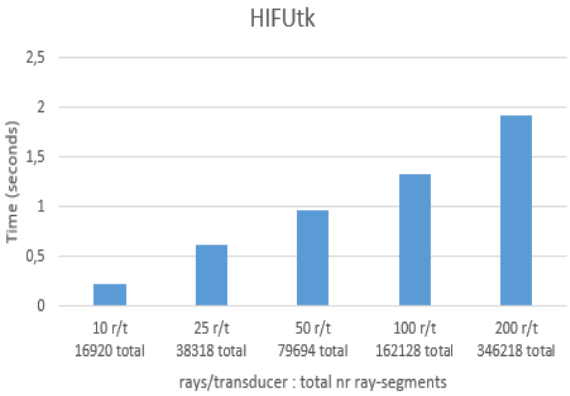

Figure 9: *Time performance from HIFUtk implementation varying the number of rays per transducer element.*

5.2. Experiments with HIFUtk

The experiment simulation pipeline is not static and can be adapted by the user. An example of such a dynamic experiment configuration is shown in Figure 10. Each of the blocks shown in Figure 10 is a component in the simulation and visualization pipeline. Each component can have one or multiple dependencies that have to be executed before it. For example the geometry needs to be generated before the Ray-tracer is executed, similarly the Ray-tracer model before the bio-heat simulation. Therefore, the application automatically constructs a dependency graph of all the components in the pipeline, keeping track of which objects have to be invalidated at each step.

5.3. Use case: rabbit bone

In this section we illustrate the use of HIFUtk by applying HIFU to a rabbit bone. We demonstrate the use of HIFUtk focusing on two common research questions. The first one is investigating the relation between the CEM shape and the focal point position. The second one is studying the effects of shear waves on the temperature distribution in bone.

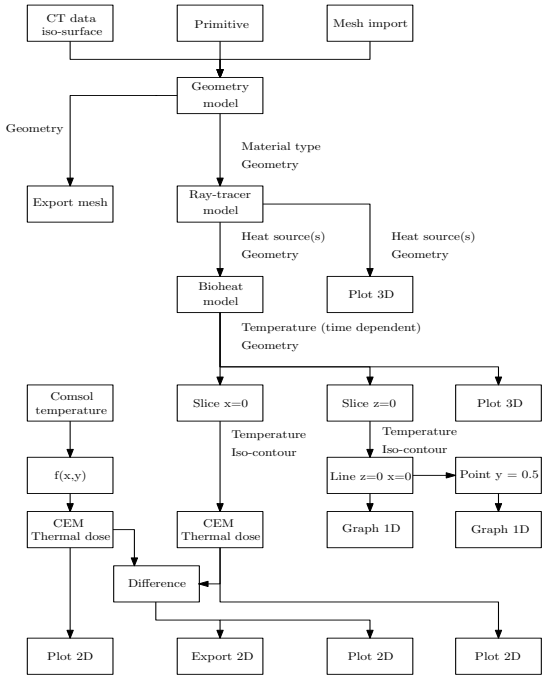

Figure 10: *Example of experiment configuration. In general, the user is able to generate data from the simulation itself, but also import data from files. Then the user is able to do logical operations on the variables stored (e.g. the block 'difference') and finally to export data.*

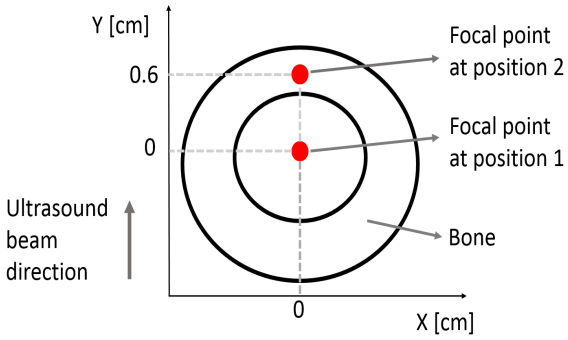

Figure 11: *The two different positions of the focal point applied to the rabbit bone.*

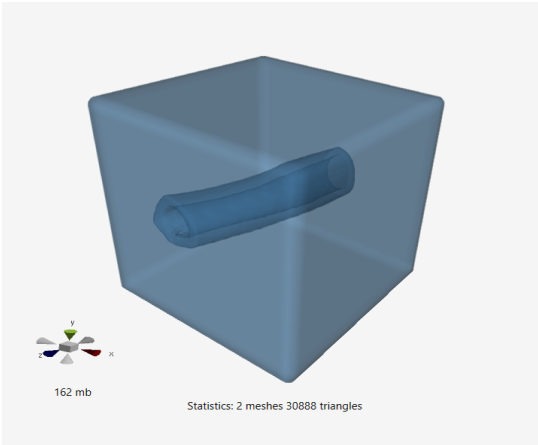

Figure 12: *Visualization of the rabbit bone geometry. The bone is surronded by a cube of soft tissue.*

5.3.1. The shift of the focal point

The goal of an effective treatment on bone is to limit the ablated region in the soft tissue around the bone. The volume of the ablated soft tissue depends on the focal point position. Therefore, in this scenario, the research question is: 'how does the ablated region change shape when varying the focal point position?'. Thus, as a first step, we compute two HIFU simulations using two different focal point positions, one at the center of the bone (position 1) and one shifted 6 *mm* (position 2) (see Figure 11). The ablated region is found computing the thermal dose (CEM) in the volume, which is dependent on the temperature output. The results of the first simulation are exported in a file, which is then imported in HIFUtk when the second simulation is computed. It is important to underline that *in vivo* experiments using HIFU systems in this case are clearly not feasible: the bone would have been compromised after the first ablation.

Geometry and parameters definition. We assume that the geometry of the bone is already given by segmentation. As the interface between the lossless oil (in which the transducer elements are immersed) and the soft tissue around the bone is flat, the soft tissue is modelled as a cube without losing in realism. The final geometry is shown in Figure 12. For each of the two components (bone and cube) we define the material parameters, like attenuation coefficient, speed of sound and density. A 3D view of the geometry is available together with 2D views of the coronal, sagittal and lateral planes.

Running the simulation To compute the thermal dose (CEM) we need both the power produced and the temperature evolution. Therefore, we set up both the Ray-tracer model and the Bioheat model (see Figure 10). In the Ray-tracer model block we specify the simulation parameters like the input power or the focal point position, as well as the model parameters like the grid size of the result variables or the number of rays per transducer element. The focal point position from one simulation to the other is changed simply modifying the focal point offset. The user can compute different simulations changing the focal point position without defin-

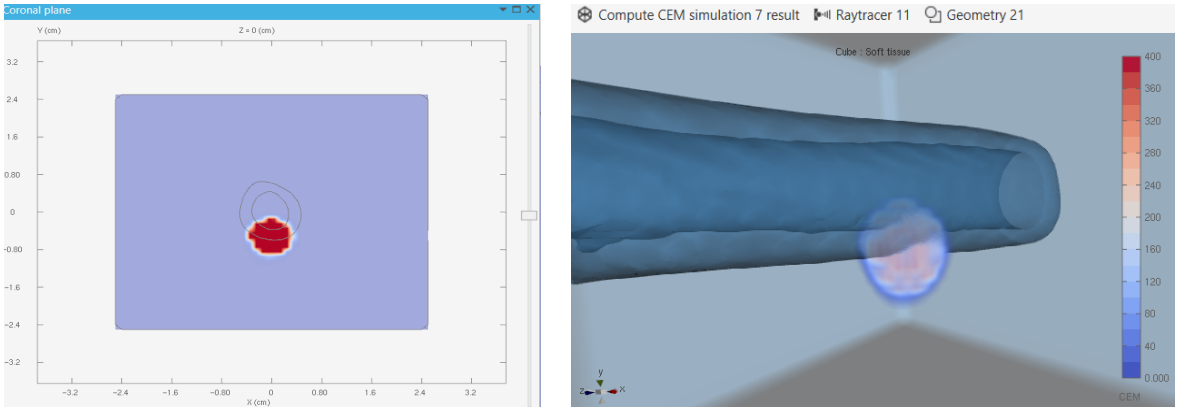

(a) (b)

Figure 13: *Result of the CEM computations in the coronal plane (a) when the focal point is at position* 1. *The red region describes the ablated tissue. Result of the CEM computations in the volume in the same configuration (b). The ablated region is not confined to the bone tissue, but also affects a part of the tissue-mimicking gel. In a clinical context, this case should be avoided.*

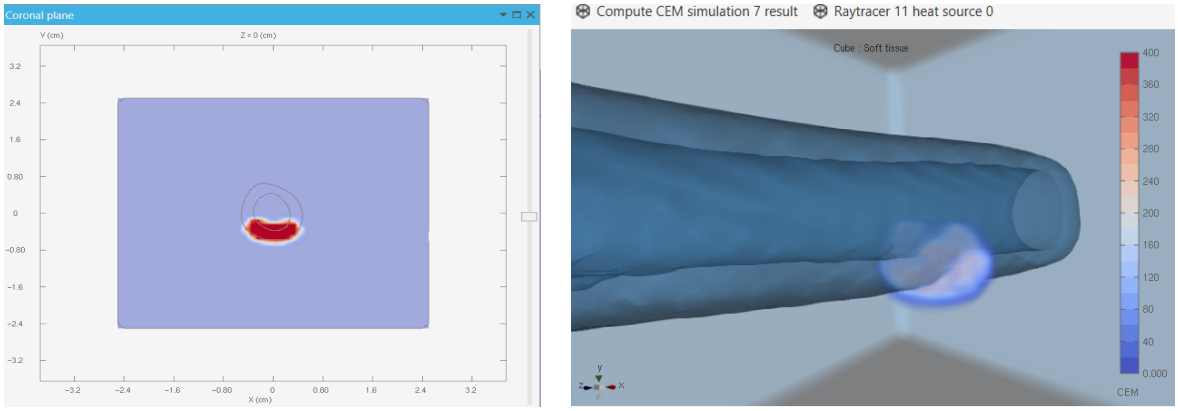

(a) (b)

Figure 14: *Result of the CEM computations in the coronal plane (a) when the focal point is at position* 2. *The red region describes the ablated tissue. Result of the CEM computations in the volume in the same configuration (b). The ablated region appears to be more confined to the bone tissue, comparing the case when the focal point is at position* 1.

ing the geometry and the experimental parameters multiple times, as it happened in the previous version of the workflow. In the Bio-heat model block we specify the bio-heat equation solver and the boundary conditions, as well as the sonication time (the treatment duration).

Once a simulation is computed, the user is able to analyse the resulting spatial data. The user is able to cut slices, lines or point from a data-set in the model editor, and every data reduction is visualized also in the data view-port (the green area in Figure 8). Every data reduction can be identified by name just by hovering the mouse over it, and the position of the slices, lines or points can be modified by dragging them using the translation tool. To investigate the effect of the focal point shift, 3D and 2D views of the ablated region are computed. The 3D views give an overview of the overall ablated volume, e.g. how big the ablated region is compared to the dimensions of the bone and the soft tissue. More details can be seen in the 2D views, such as the exact dimensions of the ablated tissue-mimicking gel around the bone. The focal point at position 1 gives an elongated ablated region as shown in Figure 13. When the focal point is at position 2 the ablated region is much more centred around the bone (see Figure 14). This case is preferable because the heating in the surrounding tissues is reduced during the ablation procedure.

5.3.2. The effects of shear waves

As bone is a solid material, both shear and longitudinal waves have to be taken into account. The contribution of shear waves depends on the inclination of the US waves when they hit the bone, as well as the shape of the geometry. A common research question is how much the shear waves affect the temperature evolution in bone. Using HIFUtk, it is possible to enable and disable the shear wave computation in the case of solid materials. In order to study how the

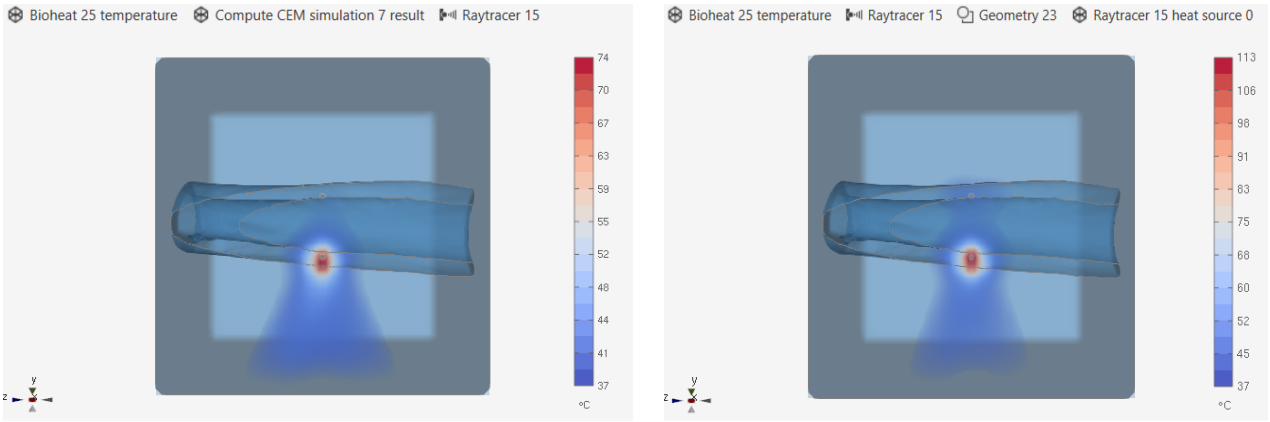

(a) (b)

Figure 15: *Temperature in the last instant of the treatment when shear waves are disabled (a) and enabled (b). Shear waves propagation increase the maximum temperature, but the focal point does not change its position.*

temperature evolution changes depending on the shear waves, we compute two simulations, both considering and ignoring the shear wave propagation in bone. As we want to investigate the position of the focal region and the variation of the maximum temperature in the hottest point, we compute the temperature in the saggittal slice in a 3D view. Doing so, we get the spatial information about the focal region (where it is located in the bone) as well as the maximum temperature reached in the focal plane. Figure 15 shows the results. The position of the focal region does not vary, but the presence of shear waves increase substantially the maximum temperature reached in the bone (from 74°C to 113°C).

5.3.3. Other research questions

Once the geometry for one experiment is defined, it is easy to obtain different results by changing parameters and re-computing the simulation. For instance, results for different input power or duration of the treatment may be obtained without defining the entire simulation set-up. This makes HIFUtk an advantageous tool for investigating the effects of HIFU in various types of materials.

6. Implementation

The back-end of the application is written in C++, the front end in C# with a WPF XAML user interface and the middle layer communicating between the two is written in C++ CLI (Common Language Infrastructure). Rendering is performed using OpenGL and GLSL shaders, GPU acceleration is achieved using NVIDIA CUDA GPU computing.

7. Conclusion and Future work

We have introduced HIFUtk, a visual analytics environment to define, perform, and visualize HIFU simulations. Our application allows researchers to get insight into the propagation of ultrasound waves and temperature development on any geometry ranging from simple primitives to surfaces extracted from CT data. Using HIFUtk, a researcher is able to compute simulations in seconds, and access and visualize all final and intermediate results. Moreover, computing simulations under varying input parameters can be done without defining the experimental set-up multiple times. The simulation results can be analyzed and compared in multiple linked views. Since HIFUtk operates stand-alone, and does not depend on third party software, researchers are now able to perform their (numerical) experiments faster, and can more easily compare model simulation results to real data from sensors or PRFS thermometry.

In future work, a dedicated comparison component will be added to the tool. It will facilitate the comparison between stored variables, without the necessity to export results. HIFUtk has researchers who develop computational models for HIFU propagation as its main target users. In future work, we plan to extend our work to a clinical environment, so that it can be used in a pre-treatment planning scenario.

References

[ATP*03] AUBRY J.-F., TANTER M., PERNOT M., THOMAS J.-L., FINK M.: Experimental demonstration of noninvasive transskull adaptive focusing based on prior computed tomography scans. *The Journal of the Acoustical Society of America 113*, 1 (2003), 84–93. doi:10.1121/1.1529663. 2

[AWR*06] AMIN V., WU L., ROBERTS R., THOMPSON R. B., RYKEN T.: HIFU therapy planning using pre-treatment imaging and simulation. In *AIP Conference Proceedings* (2006), vol. 829, pp. 206–210. doi:10.1063/1.2205467. 2

[Cob07] COBBOLD R. S. C.: *Foundations of biomedical ultrasound*. Oxford University Press, 2007. 2

[CSG74] CHAN A. K., SIGELMANN R. A., GUY A. W.: Calculations Of Therapeutic Heat Generated by Ultrasound in Fat-Muscle-Bone Layers. *IEEE Transactions on Biomedical Engineering BME-21*, 4 (1974), 280–284. doi:10.1109/tbme.1974.324314. 2

[EBE*16] EIKELDER H. M. M. T., BOŠNAČKI D., ELEVELT A., DONATO K., TULLIO A. D., BREUER B. J. T., WIJK J. H. V., DIJK E. V. M. V., MODENA D., YEO S. Y., AL. E.: Modelling the temperature evolution of bone under high intensity focused ultrasound. *Physics in Medicine and Biology 61*, 4 (aug 2016), 1810–1828. doi:10.1088/0031-9155/61/4/1810. 1, 2, 3

[Eve01] EVERITT C.: Interactive Order-Independent Transparency. *Engineering 2*, 6 (2001), 7. URL: http://citeseerx.ist.psu.edu/viewdoc/download?doi=10.1.1.18.9286{&}rep=rep1{&}type=pdf, doi:10.1111/j.1467-8659.1995.cgf143_0271.x. 4

[Haa11] HAAR G. T.: Principles of High-Intensity Focused Ultrasound. *Interventional Oncology* (2011), 51–63. doi:10.1007/978-1-4419-1469-9_5. 1

[HLB*14] HUISMAN M., LAM M. K., BARTELS L. W., NIJENHUIS R. J., MOONEN C. T., KNUTTEL F. M., VERKOOIJEN H. M., VAN VULPEN M., VAN DEN BOSCH M. A.: Feasibility of volumetric MRI-guided high intensity focused ultrasound (MR-HIFU) for painful bone metastases. *Journal of Therapeutic Ultrasound 2*, 1 (2014), 16. URL: http://jtultrasound.biomedcentral.com/articles/10.1186/2050-5736-2-16, doi:10.1186/2050-5736-2-16. 1

[HPKF12] HIPP E., PARTANEN A., KARCZMAR G. S., FAN X.: Safety limitations of MR-HIFU treatment near interfaces: a phantom validation. *Journal of Applied Clinical Medical Physics 13*, 2 (2012), 168–175. doi:10.1120/jacmp.v13i2.3739. 2

[KHM*98] KLOSOWSKI J. T., HELD M., MITCHELL J. S. B., SOWIZRAL H., ZIKAN K.: Efficient collision detection using bounding volume hierarchies of k-DOPs. *IEEE Transactions on Visualization and Computer Graphics 4*, 1 (1998), 21–36. doi:10.1109/2945.675649. 4

[KVG*14] KOSKELA J., VAHALA E., GREEF M. D., LAFITTE L. P., RIES M.: Stochastic ray tracing for simulation of high intensity focal ultrasound therapy. *The Journal of the Acoustical Society of America 136*, 3 (2014), 1430–1440. doi:10.1121/1.4892768. 2

[LGS*09] LAUTERBACH C., GARLAND M., SENGUPTA S., LUEBKE D., MANOCHA D.: Fast BVH construction on GPUs. *Computer Graphics Forum 28*, 2 (2009), 375–384. doi:10.1111/j.1467-8659.2009.01377.x. 4

[LLC*00] LIN W.-L., LIAUH C.-T., CHEN Y.-Y., LIU H.-C., SHIEH M.-J.: Theoretical study of temperature elevation at muscle/bone interface during ultrasound hyperthermia. *Medical Physics 27*, 5 (2000), 1131–1140. doi:10.1118/1.598979. 2

[LYL*00] LU B.-Y., YANG R.-S., LIN W.-L., CHENG K.-S., WANG C.-Y., KUO T.-S.: Theoretical study of convergent ultrasound hyperthermia for treating bone tumors. *Medical Engineering & Physics 22*, 4 (2000), 253–263. doi:10.1016/s1350-4533(00)00031-x. 2

[MT05] MÖLLER T., TRUMBORE B.: Fast, Minimum Storage Ray/Triangle Intersection. *ACM SIGGRAPH 2005 Courses*, 1 (2005), 1–7. doi:10.1145/1198555.1198746. 4

[NAM*13] NAPOLI A., ANZIDEI M., MARINCOLA B. C., BRACHETTI G., NOCE V., BONI F., BERTACCINI L., PASSARIELLO R., CATALANO C.: MR Imaging-guided Focused Ultrasound for Treatment of Bone Metastasis. *RadioGraphics 33*, 6 (2013), 1555–1568. doi:10.1148/rg.336125162. 1

[NM10] NELL D. M., MYERS M. R.: Thermal effects generated by high-intensity focused ultrasound beams at normal incidence to a bone surface. *The Journal of the Acoustical Society of America 127*, 1 (2010), 549–559. doi:10.1121/1.3257547. 2

[SBD*13] SCHLESINGER D., BENEDICT S., DIEDERICH C., GEDROYC W., KLIBANOV A., LARNER J.: MR-guided focused ultrasound surgery, present and future. *Medical Physics 40*, 8 (nov 2013), 80901. doi:10.1118/1.4811136. 1

[SD84] SAPARETO S. A., DEWEY W. C.: Thermal dose determination in cancer therapy. *International Journal of Radiation Oncology*Biology*Physics 10*, 6 (1984), 787–800. doi:10.1016/0360-3016(84)90379-1. 3

[SGT*03] STEWART E. A., GEDROYC W. M., TEMPANY C. M., QUADE B. J., INBAR Y., EHRENSTEIN T., SHUSHAN A., HINDLEY J. T., GOLDIN R. D., DAVID M., AL. E.: Focused ultrasound treatment of uterine fibroid tumors: Safety and feasibility of a noninvasive thermoablative technique. *American Journal of Obstetrics and Gynecology 189*, 1 (2003), 48–54. doi:10.1067/mob.2003.345. 1

[Son09] SONESON J. E.: A user-friendly software package for HIFU simulation. In *AIP Conference Proceedings* (2009), vol. 1113, pp. 165–169. doi:10.1063/1.3131405. 2

[SPS*13] SCOTT S. J., PRAKASH P., SALGAONKAR V., JONES P. D., CAM R. N., HAN M., RIEKE V., BURDETTE E. C., DIEDERICH C. J.: Interstitial ultrasound ablation of tumors within or adjacent to bone: Contributions of preferential heating at the bone surface. *Energy-based Treatment of Tissue and Assessment VII* (2013). doi:10.1117/12.2002632. 2

[SQM05] SENNEVILLE B. D. D., QUESSON B., MOONEN C. T. W.: Magnetic resonance temperature imaging. *International Journal of Hyperthermia 21*, 6 (2005), 515–531. doi:10.1080/02656730500133785. 1

[SRT*06] STEWART E. A., RABINOVICI J., TEMPANY C. M., INBAR Y., REGAN L., GASTOUT B., HESLEY G., KIM H. S., HENGST S., GEDROYE W. M., AL. E.: Clinical outcomes of focused ultrasound surgery for the treatment of uterine fibroids. *Fertility and Sterility 85*, 1 (2006), 22–29. doi:10.1016/j.fertnstert.2005.04.072. 1

[SSP*14] SCOTT S. J., SALGAONKAR V., PRAKASH P., BURDETTE E. C., DIEDERICH C. J.: Interstitial ultrasound ablation of vertebral and paraspinal tumours: parametric and patient-specific simulations. *International journal of hyperthermia : the official journal of European Society for Hyperthermic Oncology, North American Hyperthermia Group 30*, 4 (2014), 228–244. arXiv:15334406, doi:10.3109/02656736.2014.915992. 2

[Tho95] THOMAS J. W.: *Numerical Partial Differential Equations: Finite Difference Methods*, vol. 22. 1995. URL: http://link.springer.com/10.1007/978-1-4899-7278-1, arXiv:arXiv:1011.1669v3, doi:10.1007/978-1-4899-7278-1. 4

[TJRC12] TREEBY B. E., JAROS J., RENDELL A. P., COX B. T.: Modeling nonlinear ultrasound propagation in heterogeneous media with power law absorption using a k-space pseudospectral method. *The Journal of the Acoustical Society of America 131*, 6 (2012), 4324–36. URL: http://www.ncbi.nlm.nih.gov/pubmed/22712907, doi:10.1121/1.4712021. 2

[VC12] VYAS U., CHRISTENSEN D.: Ultrasound beam simulations in inhomogeneous tissue geometries using the hybrid angular spectrum method. *IEEE Transactions on Ultrasonics, Ferroelectrics and Frequency Control 59*, 6 (2012), 1093–1100. doi:10.1109/tuffc.2012.2300. 2

[VFW*00] VAEZY S., FUJIMOTO V. Y., WALKER C., MARTIN R. W., CHI E. Y., CRUM L. A.: Treatment of uterine fibroid tumors in a nude mouse model using high-intensity focused ultrasound. *American Journal of Obstetrics and Gynecology 183*, 1 (2000), 6–11. doi:10.1067/mob.2000.105347. 1

[VSP*] VILLARD C., SOLER L., PAPIER N., AGNUS V., GANGI A., MUTTER D., MARESCAUX J.: RF-Sim: a treatment planning tool for radiofrequency ablation of hepatic tumors. *Proceedings on Seventh International Conference on Information Visualization, 2003. IV 2003.* doi:10.1109/iv.2003.1218041. 2

[WARR07] WU L., AMIN V., ROBERTS R., RYKEN T.: An Interactive HIFU Therapy Planning Using Simulation & Visualization. *AIP Conference Proceedings* (2007). doi:10.1063/1.2744266. 2

[WMA*] WOJCIK G., MOULD J., ABBOUD N., OSTROMOGILSKY M., VAUGHAN D.: Nonlinear modeling of therapeutic ultrasound. *1995 IEEE Ultrasonics Symposium. Proceedings. An International Symposium*. doi:10.1109/ultsym.1995.495865. 2

[ZJOB10] ZHAO B., JOINER M. C., ORTON C. G., BURMEISTER J.: "SABER": A new software tool for radiotherapy treatment plan evaluation. *Medical Physics 37*, 11 (jun 2010), 5586–5592. doi:10.1118/1.3497152. 2